wjpmr, 2017,3(9), 238-245

SJIF Impact Factor: 4.103

WORLD JOURNAL OF PHARMACEUTICAL AND MEDICAL RESEARCH
www.wjpmr.com

Research Article
ISSN 2455-3301
WJPMR

EXPLORING THE COORDINATION CAPABILITIES, THERMAL AND ANTIMICROBIAL STUDIES OF 1-PHENYL-3-METHYL-4-BENZOYL-5-PYRAZOLONE N (4)- METHYL- N(4)-PHENYLTHIOSEMICARBAZONE

K. G. Sangeetha* and K. K. Aravindakshan

Department of Chemistry, University of Calicut, 673635, Kerala, India.

***Corresponding Author: K. G. Sangeetha**
Department of Chemistry, University of Calicut, 673635, Kerala, India.

Article Received on 09/08/2017 **Article Revised on 29/08/2017** **Article Accepted on 19/09/2017**

ABSTRACT

Transition metal complexes of an ONS donor ligand, 1-phenyl-3-methyl-4-benzoyl-5-pyrazolone, N(4)-methyl-N(4)-phenylthiosemicarbazone (H_2L) were synthesised. The metal complexes were characterized by elemental analyses, magnetic susceptibility measurements, electronic, vibrational and ^{1}H-NMR spectra. ESR spectrum of the copper(II) complex was recorded. Thermal stabilities of the complexes were also ascertained. The preliminary *in vitro* antimicrobial screening of the ligand, copper and zinc complexes were also performed. For this studies, four fungal strains, three Gram (-ve) and three Gram (+ve) bacteria were used. Complexes showed better microbial inhibition activity than the ligand.

KEYWORDS: N(4)-Methyl-N(4)-phenylthiosemicarbazide, 1-phenyl-3-methyl-4-benzoyl-5- pyrazolone, complexes, magnetic susceptibility.

INTRODUCTION

Thiosemicarbazones are considered as one of the most vital scaffolds and are embedded in many biologically active compounds. They belong to the family of thiourea derivatives. Parent aldehyde or ketone moiety in the compound has a substantial role towards its biological property. Metal complexes of thiosemicarbazones show more activity than the free ligands.[1] A mesmerizing feature of thiosemicarbazones is that, they generally exist in the thioketo form in the solid state, while in solution state, they display a thioketo- thioenol tautomerism. In thioketo form they act as a neutral bidentate ligands and the enol form they deprotonate and act as monoanionic bidentate ligand towards metal ions. They can exist in *E* form (*trans*-) and Z form (cis-).[2] In *E* form they will act as monodentate ligands by coordinating through the sulphur atom alone. If the sulfur centre is substituted, the bonding may occur through the hydrazine nitrogen and the amide nitrogen atoms. Generally, the compound is in the *Z*-form while coordinating to the metal ions and is attributed to the chelate effect on complexation. When an extra coordination site is present near to the donating centres, they will coordinate in a tridentate manner.

Studies showed that the substitutions at the terminal positions of thiosemicarbazones have much improved their anticancer activity.[3] Biological properties are enhanced when these molecules are substituted at the 4th nitrogen. The presence of phenyl group at N(4) position of isatin-β thiosemicarbazones derivatives exposed increased cytotoxicity against the parental KB-3-1 cell lines and the P-glycoprotein-expressing cell line KB-V1.[4,5]

Pyrazolone derivatives are used as starting materials for the synthesis of biologically active compounds and for the construction of condensed heterocyclic systems.[6] They are found to exhibit keto-enol tautomerism. Yuting Zhong *et al.*[7] reported the crystal structure and photoisomerism of 1-phenyl-3-methyl-4-(4-fluorobenzal)-5-pyrazolone 4-methylthiosemicarbazone in the solid state. However, pyrazolone-based thiosemicarbazone chemistry is less extensive.

For a last few decades, we have been in constant hunt of the synthesis and structural characterization of a variety of Schiff bases with the aim to correlate their structure with chelating ability and biological activity.[8,9] It is found that most of the microbes are resistant towards the available antibiotics. So there is a crucial need for the development of new and useful antimicrobial agents. Therefore, designing antimicrobial agents which are distinct from those of the classical antibiotics becomes one of the main aims of our current study.

So we focused on the synthesis of thiosemicarbazones with disubstitution at N(4) position (methyl and phenyl groups). The current study describes the syntheses of 1-phenyl-3-methyl-4-benzoyl-5-pyrazolone N(4)-methyl-

N(4)-phenylthiosemicarbazone (H_2L), their nine transition metal complexes and their spectral, thermal and *in vitro* antimicrobial properties.

EXPERIMENTAL

Materials

N(4)-Methyl-N(4)-phenylthiosemicarbazide was prepared according to the reported procedure.[10] 1-Phenyl-3-methyl-4-benzoyl-5-pyrazolone was prepared by using Jenson's method.[11]. Commercially available metal salts were used without further purification. The solvents were purified and dried according to the standard procedures.

Preparation

Preparation of 1-phenyl-3-methyl-4-benzoyl-5-pyrazolone N (4)-methyl-N (4)-Phenylthiosemicarbazone

The ligand was prepared by stirring the hot methanolic solution of 1- phenyl-3-methyl-4-benzoyl-5-pyrazolone (PMBP) (750mg, 2.76mmol) and N (4)-methyl-N (4)-

Phenylthiosemicarbazide (MPTSC) (500mg, 2.76mmol) on a magnetic stirrer, followed by refluxing at 60-80^{o}C for 30 minutes. The ligand formed was filtered and washed with methanol and dried over anhydrous $CaCl_2$. The suggested empirical formula for the ligand is $C_{25}H_{23}N_5OS$.

General procedure for the preparation of metal complexes

Ligand (H_2L) (1mmol) was dissolved in two or three drops of chloroform and excess of hot methanol. To this solution, metal salt (1mmol) dissolved in hot water/ hot methanol was added dropwise and refluxed for 3-4 h. The precipitate formed was filtered. It was then washed with water followed by methanol and dried over $CaCl_2$ in a desiccator.

Physicochemical techniques

Elemental analyses were performed on EURO VECTOR CHNS analyser Model No: EA 3000. Electronic spectra were recorded on JascoV-550 UV-Vis spectrometer. Infrared (IR) spectra were recorded on a Jasco-FT-IR-4100 model spectrometer using KBr pellets. NMR was recorded on 400MHz BrukerAvance111 FT NMR spectrometer. The magnetic susceptibilities of the complexes at room temperature were measured using Sherwood Scientific Magnetic Susceptibility Balance. Diamagnetic corrections were made using Pascal's constants for all atoms and bonds. TG was recorded on TGA Q50 V20.13 Build 39 model thermo gravimetric analyzer fitted with a thermal analysis controller. DSC of the ligand was recorded on a Perkin Elmer DSC apparatus 4000 series. The ESR spectrum of copper complex was recorded on FA200 ESR instrument calibrated with Mn^{2+} marker. The melting points of the ligand and complexes were determined using a melting point apparatus.

Procedure for antimicrobial studies

Antibacterial studies

The synthetized compounds were tested *in vitro* for their antibacterial activity against Gram positive and Gram-negative organisms by Kirby–Bauer agar diffusion method.[12] Mueller–Hinton agar medium was used in this method. The bacterial strains used were *Staphylococcus aureus* (MTCC 3160), *Enterococcus faecalis*, *Bacillus subtili* (MTCC-619), *E.coli* (MTCC 4296), *pseudomonas aeruginosa* (MTCC 2488) and *Klebsiella Pneumonia*. Muller Hinton Agar plates were prepared and the test microorganisms were inoculated by the spread plate method. Filter paper discs, approximately 6 mm in diameter, were soaked with 10µl of the test substance. It is allowed to dry and placed in the previously prepared agar plates. Each disc was pressed down to ensure complete contact with the agar surface and distributed evenly so that they are no closer than 24 mm (center to center) from each other. The agar plates were then incubated at 37ºC. After 16 to 18 hours of incubation, each plate was examined. The activity was measured by calculating the diameter of the inhibition zone (in mm). Standard antibiotics, Kanamycin and Ampicillin (10 µg/disc), were used as the positive control. DMSO was used as a negative control under the same conditions for each organism and no activity was found. The activity results were calculated as a mean of triplicates. Dilution susceptibility testing methods were used to determine the minimal concentration of antimicrobial needed to inhibit or kill the microorganism. The test compounds were diluted to get a series of concentrations from 2000 ppm to 0.315 ppm in seven test tubes. The microorganism suspension of 500µl was added to the broth dilutions. In control 1, added culture and broth and in control 2 added the compound and broth. These were incubated for 18 hours at 37ºC. MIC of each sample was taken as the lowest concentration that did not give any visible bacterial growth.

Antifungal studies

The antifungal activities of the ligand and complexes were tested against *Alternaria alternata* MTCC 2724, *Aspergillus* niger (MTCC282), *Colletotrichum gloeosporioides* (MTCC 3439), *Candida Albicans* ((MTCC 227) using Potato-Dextrose agar medium(PDA).[13] This is having the composition, potato 200g, dextrose 20 g, agar–agar 20 g and distilled water 1000 ml. To the molten PDA medium, requisite amount of the ligand was added after being dissolved in DMSO to get certain concentrations (20 to 60 ppm). The amended medium then was poured into sterile Petri plates and allowed to solidify. After solidification, 5mm diameter mycelia discs were taken from the actively growing 48hrs old culture by using a sterile cork borer and placed on the medium with the help of inoculum's needle. For the control, the discs were inoculated on PDA medium without the ligand. These Petri plates were placed in an incubator at room temperature. Triplicates were used in each case. The diametrical growth of the fungus was recorded in each Petri plate and average

growth of the fungal colony after 72 h and the percentage inhibition was calculated by the equation: Percentage inhibition = C-T x 100/C, where *C* and *T* are the diameters of the fungal colony in the control and the test plates, respectively.

RESULTS AND DISCUSSION

Formulae and general properties of the ligand

The empirical formula, melting point, colour, partial elemental analyses and magnetic moments of the ligand and its metal complexes are depicted in Table 1.

The ligand and all the complexes were found to be stable at room temperature. The colour of all the complexes indicate the presence of sulfur-to-metal charge-transfer transitions.[14] In complexes, the ligand coordinates in dianionic(L^{2-}), monoanionic (HL^-) or neutral (HL_2) form. Elemental analyses values were in good harmony with the proposed empirical formula.

Table 1: The empirical formula, melting point, colour, partial elemental analyses, and magnetic moments of the ligand and its metal complexes.

Complex No:	Compound	M.W	M.P	Colour	Yield	Elemental Analysis Found(calculated)					μ in BM
						C	H	N	S	M	
	$C_{25}H_{23}N_5OS$	442	163	Yellow	80	68.2 (68.0)	5.2 (5.0)	15.9 (15.9)	7.2 (7.3)	–	–
1	$[NiHLCH_3COO]$	559	225	brown	70	53.5 (53.6)	4.0 (4.2)	12.5 (12.5)	6.0 (5.7)	10.3 (10.5)	D
2	$[Ni(HL)_2]H_2O$	960	204	light green	70	62.4 (62.5)	4.8 (4.6)	14.8 (14.6)	7.0 (6.7)	5.8 (5.8)	2.7
3	$[Cu(HL)_2]H_2O$	965	203	green	80	62.2 (62.2)	4.6 (4.8)	14.5 (14.5)	6.8 (6.6)	6.8 (6.6)	2.1
4	[Cu(HL)Cl]	541	230	dark green	80	55.7 (55.5)	3.7 (4.0)	12.8 (12.9)	5.8 (5.9)	11.9 (11.7)	1.7
5	$[Cu(HL)NO_3]$	568	215	green	80	52.8 (52.8)	3.7 (3.9)	12.0 (12.3)	5.8 (5.6)	10.9 (11.1)	1.7
6	$[(CuHL)_2(OH)_2]$ $5H_2O$	1135	195	green	70	53.0 (52.7)	4.7 (4.9)	12.1 (12.3)	5.8 (5.6)	10.9 (11.1)	D
7	$[Zn(HL)_2]$	948	190	yellow	80	63.3 (63.4)	4.6 (4.6)	14.6 (14.8)	7.0 (6.8)	6.9 (6.9)	D
8	$[(ZnHL)_2(NO_3)_2]$ $2H_2O$	1174	130	yellow	80	51.0 (51.1)	4.0 (4.0)	14.0 (14.3)	5.3 (5.4)	11.2 (11.1)	D
9	$[(ZnHL)_2(OH)_2]$ $2H_2O$	1138	178	yellow	70	52.7 (52.7)	4.6 (4.9)	12.2 (12.3)	5.7 (5.6)	11.4 (11.5)	D

Electronic spectra and magnetic moment

The electronic spectrum of ligand registered bands at 259, 321 and 425 nm in the solid state. The complexes have bands in the range 250-260 and 320-360 nm, which are due to $\pi \rightarrow \pi^*$ and $n \rightarrow \pi^*$ transitions. Additonal bands were observed in the range 350-390 nm in the spectra of complexes. These may be due to sulphur to metal charge-transfer transitions.

Ni (II) complex (1) showed a single broad band at 509 nm could be assigned to $^1A_{1g} \rightarrow {}^1B_{1g}$ transition. This is consistent with square planar geometry.[15] For the complex (2), broad bands at 873 nm, due to $^3A_{2g} \rightarrow {}^3T_{2g}(F)$ and 590 nm, due to $^3A_{2g} \rightarrow {}^3T_{1g}(F)$ transitions were observed. The broad band between 330-410 nm may be assigned for charge-transfer as well as to the $^3A_{2g}$ (F) $\rightarrow {}^3T_{1g}$ (P) transitions and is consistent with the octahedral geometry.

The broad band observed at 532 nm in the complex (3) is assigned to $^2E_g \rightarrow {}^2T_{2g}$ transition. This is in agreement with the octahedral geometry of this complex.

The coordinated anions, X-Cu (II) charge-transfer was observed at 400-500 nm. For the complex 4, the Cl-Cu (II) charge-transfer band was found at 488 nm. In the complex (5), the O-Cu (II) charge-transfer band was observed at 419 nm. Complexes (4), (5) and (6) have broad d-d combination bands in the range 666-588 cm^{-1} and appear as a shoulder on the intraligand and charge transfer bands. In accordance with previous observation, such an attribute is expected for a square planar Cu (II) complex.

As expected zinc complexes shows band almost similar to the ligand. The electronic spectral data of the ligand and the complexes are shown in Table 2.

[NiHLCH$_3$COO] (1) is diamagnetic with square planar geometry. The magnetic moment of complex (2) is 2.7 B.M. and supports its octahedral geometry. The complex (3) shows magnetic moment value 2.1 B.M. supporting its distorted octahedral structure. The magnetic moment values of the complexes (4) and (5) are found to be 1.70 B.M., respectively, and support their square planar structure. The copper (II) complex, (6) is found to be diamagnetic which is in accordance with the dimeric nature. This may be due to the strong antiferromagnetic interaction between the adjacent copper(II) ions. The zinc(II) complexes are found to be diamagnetic.

Table 2: Electronic spectral data of the ligand and complexes (nm).

Complex No:	Compound	Intraligand and CT bands(nm)	d-d bands (nm)
	H_2L	256 ,321, 425	-
1	[Ni(HL)CH_3COO]	338	509
2	[Ni$(HL)_2$] H_2O	254, 283, 340	330-410, 590, 873
3	[Cu$(HL)_2$.H_2O	260, 343, 386	533
4	[Cu(HL)Cl]	259,302,334, 353, 489	646
5	[Cu(HL)NO_3]	260, 328, 419	600, 889
6	[$(CuHL)_2(OH)_2$] $5H_2O$	252,305,327, 431	598
7	[Zn$(HL)_2$]	259, 409	-
8	[$(ZnHL)_2(NO_3)_2$] $2H_2O$	354, 416	-
9	[$(ZnHL)_2(OH)_2$] $2H_2O$	263,	350, 414

FT-IR Spectra

The IR spectral data of the ligand and the complexes are shown in Table 3. The vibrations belonging to N-H stretching usually occur in the region 3450–3250 cm^{-1}.[16] The ligand shows a broad band at 3411 cm^{-1} due to ν(NH). The increase in the wavenumber of the centre of this broad band may be due to the involvement of azomethine nitrogen during the complex formation. The band due to ν(C=O) at 1626 cm^{-1} shifts to higher wavenumber on coordination with metals. The ν(N-N) band at 1106 cm^{-1} undergoes a shift to higher wavenumber in the spectra of the complexes compared to that of the ligand substantiate the involvement of azomethine nitrogen in coordination .[17] This blue shift may be due to the decrease in the repulsion between the lone pairs on the two nitrogen atoms. The ν(M-N) vibration are observed around 440-485 cm^{-1}. All these findings confirm the participation of azomethine nitrogen in coordination.

In the present case, Ni(HL)CH_3COO (1) shows band at 1519 cm^{-1} and 1430 cm^{-1} which may be due to the unidentate coordinated acetate group. Since thiols can cause spin pairing more effectively than thioethers, coordination occurs through the thiolato sulphur atom after deprotonation in this Ni(II) complex. The spectrum of nitrate complex of copper has strong bands at 1440, 1350, 1022 cm^{-1} due to $\nu_{as}(NO_2)$, $\nu_s(NO_2)$ and ν(NO), respectively, indicating the unidentate coordination of the nitrate ion to the Cu(II) ion. The separation of the two highest frequency bands is 90 cm^{-1}. The broad absorption band centred at 3400 cm^{-1} in the IR spectra of certain metal complexes has also been assigned to lattice water molecule.

Table 3: IR spectral assignments.

No:	COMPOUND	N-H/OH	C=O	CN-NH	C-O	C=S	N-N	M-O	M-N
H_2L	$C_{25}H_{23}N_5OS$	3411	1626	1478	-	1362, 831	1106	-	-
1	[NiHLCH$_3$COO]	3437		1486		1349, 850	1117	-	433
2	[Ni$(HL)_2$].H_2O	3440	1603	1489	1437	1348, 850	1107	660	472
3	[Cu$(HL)_2$].H_2O	3435	1599	1485	1439	1354, 842	1128	661	462
4	[Cu(HL)Cl]	3445	1591	1486	1416	1351	1129	663	441
5	[Cu(HL)NO_3]	3442	1592	1485	1441 1419	1372, 854	1129	662	448
6	[$(CuHL)_2(OH)_2$]$5H_2O$	3443	1598	1486		1366, 838	1128	661	453
7	[Zn$(HL)_2$]	3438	1602	1482	1434	1346, 851	1126	659	433
8	[$(ZnHL)_2(NO_3)_2$] $2H_2O$	3438	1599	1486	1437	1348, 848	1129	-	450
9	[$(ZnHL)_2(OH)_2$] $2H_2O$	3425	1602	1485	1436	1346, 849	1108	659	444

^{1}H-NMR Spectrum

The ^{1}H NMR spectrum of the zinc complexes are recorded in $CDCI_3$ (figure.1). Two singlets observed in the ligand spectrum at 14.476 ppm due to NH proton and 11.176 ppm due to OH proton were absent in zinc(II) complex. The absence of peak at 11.176 ppm is due to the deprotonation of O-H proton during complexation. Aromatic protons exhibit multiplet signals in the range 7.13-8.13 ppm. A new peak at 6.675 ppm due to N-H proton is observed. It is an evidence for the participation of thione sulphur in complexation. N-CH_3 protons in the complex show peaks at 3.4-3.64 ppm. Singlet peaks at 1.2-1.3 ppm in the complex correspond to the methyl protons in the substituted pyrazolone. Both CHNS data and NMR data are in agreement with the formulae $M(HL)_2$ for zinc(II) complex (7).

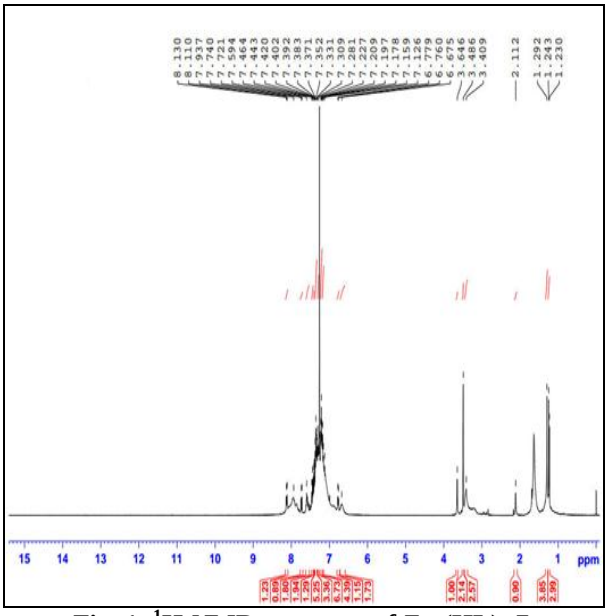

Fig. 1: ^{1}H-NMR spectrum of Zn $(HL)_2$ 7.

ESR spectrum

The ESR spectrum of copper(II) complex (3) were recorded in frozen DMF solution at 77 K in the X-band with 100 kHz field modulation and *g* factors were assigned in comparison with the standard marker Mn^{2+}. The Cu(II) ion has an effective spin of *S*=3/2. It is associated with a spin angular momentum *ms*= ±1/2, leading to a doubly degenerate spin state in the absence of magnetic field. The degeneracy is lifted between these states in a magnetic field. The energy difference between them is given by $E = hv = g\beta B$, where *h* is the Planck's constant, *v* is the frequency, *g* is the Lande's splitting factor equals to 2.0023 (for a free electron), β is the Bohr magneton and *B* is the magnetic field. The solution spectrum of the complex (3) at 77 K in DMF was axial and showed four hyperfine lines characteristic of a monomeric Cu(II) complexes corresponding to -3/2, -1/2, 1/2 and 3/2 which arise from the coupling of the odd electron with copper nuclei(I=3/2). The spectrum also gave three superhyperfine lines in the perpendicular region which arose from the coupling of the electron spin with nuclear spin of nitrogen atom which is coplanar. It indicates that in this complex azomethine nitrogen atom has coordinated to the metal centre. Since there is no half field signal, we can confirm the monomeric nature of complex (3).

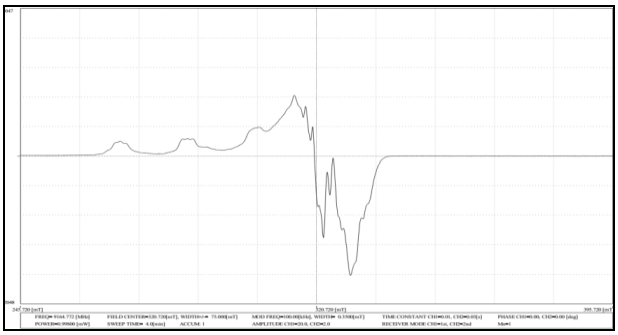

Fig. 2: ESR spectrum of Cu $(HL)_2.H_2O$ (3).

Thermal studies

The thermal studies of the ligand and metal complexes were carried out using the thermogravimetric technique (TG-DTG) in order to provide more insight into their structure of the complexes.

For the ligand H_2L, two stages of decomposition were observed and is evident from DTG peaks at 163^{o}C and 273^{o}C. The first stage of decomposition of the ligand occured at 140-170 ^{o}C, and second stage due to complete decomposition of ligand at 170-750 ^{o}C. The absence of any thermal change before this temperature demonstrates their high thermal stability. DSC plot supports the TG-DTG analysis giving temperature maxima at 163^{o}C and at 273^{o}C. The TG/DTG/DSC study reveals the purity of the compound and no decomposition is observed up to the melting point.

Ni(HL)CH_3COO (1) showed four decomposition stages. It is evident from DTG peaks at 225, 302, 310 and 321°C. Here the decomposition starts after the melting point of the compound at 225°C. The first stage is at 202–274°C and demonstrates a mass loss of 5 %, corresponding to the loss of CO (calc.5 %). The second stage occurs at 274–507 °C, with a mass loss of 39.8 %. The residual mass left behind at 745°C was 55.35 %.

$Ni(HL)_2.H_2O$ (2) has four decomposition stages are observed. It is evident from DTG peaks at 71, 204, 231 and 309°C. Initial mass loss corresponds to the loss of one lattice held water molecule. Here also the decomposition starts after the melting point of the compound at 204°C. The first stage is at 184–210°C and demonstrates a mass loss of 3.3 %. The second stage occurs at 254–649°C, with a mass loss of 70.5%. A residual mass of 17.7 % was left which may be due to the formation of a mixture of oxide and sulphide of nickel.

For $Cu(HL)_2.H_2O$ (3), an initial mass loss of 2% corresponds to loss of one water molecule in temperature range 150-170°C. The next steps of decomposition occur in the temperature range 180-250°C and 230-350°C. These steps are shown by DTG peaks at 161°C, 203°C

and 307°C. A residual mass of 23% was left which may be due to the formation of a mixture of copper oxide and copper sulphide (calc. 24.7 %).

For Cu(HL)Cl (4), a two staged decomposition occurred and is evident from DTG peaks at 231 and 300°C. The first stage is at 220–240°C, and demonstrates a mass loss of 6.5 %, corresponding to the loss of HCl (calc. 6.7%). The second stage occurs at 245–500 °C, with a mass loss of 56.9%. The residual mass left behind at 745°C was 28.6%. This may be due to the formation of Cu_2S (29.4%).

For $[Cu(HL)NO_3]$ (5), two stages of decomposition occur and is evident from DTG peaks at 214°C and 297 °C. The first stage is at 190-223°C, and demonstrates a mass loss of 6%, corresponding to the loss of NO (calc.5.3 %). The second stage occurs at 240-550°C, with a mass loss of 61%. The residual mass of 27.5 % was observed at 750°C which may be due to the formation of copper sulphide (calc.28 %).

For $[(CuHL)_2(OH)_2].5H_2O$ (6), DTG peaks are observed at 196 and 302°C indicating its two step decomposition. The first stage is at 183-216°C, and demonstrates a mass loss of 6 %. The second stage occurs at 240-467°C, with a mass loss of 47.2%. The residual mass of 34.81% was observed at 750°C which may be due to the formation of Cu_2S (calc. 34.2 %). Antimicrobial studies

The preliminary *in vitro* antibacterial screening studies of H_2L and its complexes are given in Table 4. However, the correct biochemical mechanism of such compound is not yet completely understood. The mode of action of antimicrobials may involve various targets in the microorganisms.[18]

1. By interefering during the synthesis of cellular walls, causes damage which leads to altered cell permeability characteristics or disordered lipoprotein arrangements, eventually resulting in cell death.
2. By the deactivation of a variety of cellular enzymes that play a crucial role in the metabolic pathways of these microorganisms.
3. Denaturation of cellular proteins, causing the normal cellular processes to be impaired.
4. A hydrogen bond formation through the azomethine group with the active centres of various cellular constituents, resulting in interference with normal cellular processes.

$Cu(HL)_2.H_2O$ (3) exhibited high activity towards *Staphylococcus aureus* in comparison with the standard drugs. It is observed that most of the compounds are particularly effective on *Enterococcus faecalis, pseudomonas aeruginosa* and *Klebsiella pneumonia.* They exhibited no activity against *Bacillus subtili even* at higher concentration. These observations can be assumed as selective activity. MIC value of all the complexes was found to be 0.315µg/ml.

The data in Table 5 show that the copper chloride and copper nitrate complexes are active against the fungi, *Aspergillus niger* and *Colletrotrichum gleosporides*. The percentage of inhibition is found to be 85% at 60ppm. $Cu(HL)_2.H_2O$ shows 70% inhibition towards Candida Albicans at 40 ppm. Zinc (II) complex (7) shows promising antifungal activity towards all the fungi under study whereas $[(CuHL)_2(OH)_2].5H_2O$ shows less activity against all fungi.

Table 4: Preliminary in vitro antibacterial screening studies of H_2L and its complexes.

Compound	Diametre of Zone of Inhibition(mm)					
	Staphylococcus aureus	***Enterococcus faecalis***	***Bacillus subtili***	***E.coli***	***pseudomonas aeruginosa***	***Klebsiella pneumonia***
H_2L	7	-	-	8	8	10
$Cu(HL)_2\ H_2O$	10	10	-	7	10	15
Cu(HL)Cl	7	8	-	7	7	18
$Cu(HL)NO_3$	8	7	-	7	10	18
$[(CuHL)_2(OH)_2].5H_2O$	14	8	-	-	-	8
$Zn(HL)_2$	7	10	-	8	8	11
$[(ZnHL)_2(NO_3)_2]\ 2H_2O$	-	10	-	7	7	-
Kanomycin	12	9	12	12	10	20
Methicillin	10	8	10	15	12	25
DMSO	-	-	-	-	-	-

Table 5: Preliminary in vitro antifungal screening studies of H_2L and its complexes.

Fungi	Percentage of inhibition																	
	H_2L			$Cu(HL)_2$			$Cu(HL)Cl$			$Cu(HL)NO_3$			$[(CuHL)_2(OH)_2].5H_2O$			$Zn(HL)_2$		
Conc:ppm	20	40	60	20	40	60	20	40	60	20	40	60	20	40	60	20	40	60
Aspergillus niger	38	49	48	58	60	58	44	63	85	46	48	50	33	35	35	64	60	62
Alternaria alternata	30	38	41	40	56	57	49	51	48	47	56	50	30	37	32	64	62	65
Candida Albicans	30	36	42	56	70	71	59	59	58	32	35	45	28	30	30	63	70	70
Colletrotrichum gleosporides	56	57	58	62	60	60	70	85	85	77	85	80	25	28	33	84	82	83

CONCLUSION

From the study, coordination capabilities of thiosemicarbazones are found to be unpredictable and are very interesting. We observed that with different salts of same metal, same ligand has coordinated in different modes. Nickel acetate yielded diamagnetic square planar complex with formula $M(HL)CH_3COO$ whereas nickel chloride gave paramagnetic octahedral complex, $M(HL)_2.H_2O$. Out of the four copper(II) complexes of H_2L, two have the general formula [MHLX] where X=Cl, NO_3. By using copper(II) acetate and zinc(II) acetate, H_2L yielded the complexes with general formula $[M(HL)_2]$ where M=Cu(II), Zn(II). This Cu(II) complex is diamagnetic and strongly supports its existence as a dimer in the solid state. The preliminary antimicrobial screening results revealed that the complexes showed a significant activity compared to the ligand, H_2L. The observations in our study understood a selective activity of the compounds towards microbes. At this phase, it is hard to find a simple explanation for the antimicrobial activity of the compounds and further studies will be needed to clarify these observations. The proposed structures of the complexes are given in FIGs 3, 4, 5.

As a continuation of our work on the synthesis of biologically active compounds, docking studies and *in vivo* biological activities are conducted on various transition metal complexes.

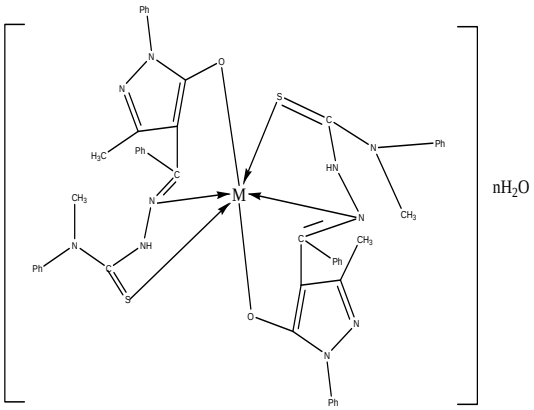

Fig. 3: Proposed structure of complex M $(HL)_2$ nH_2O (2, 3, 7).
where M = Ni(II), Cu(II), Zn(II)

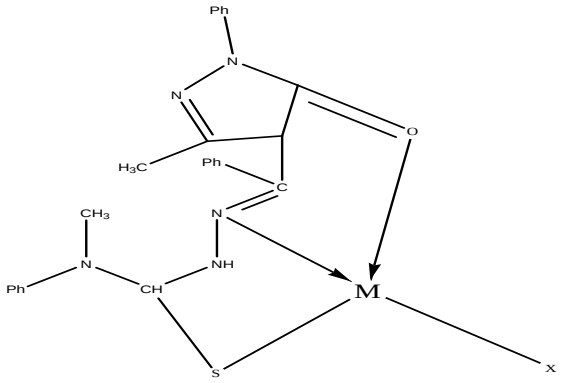

Fig. 4: Proposed structure of complex M (HL) CH_3COO.
Where M=Ni, X=CH_3COO^-

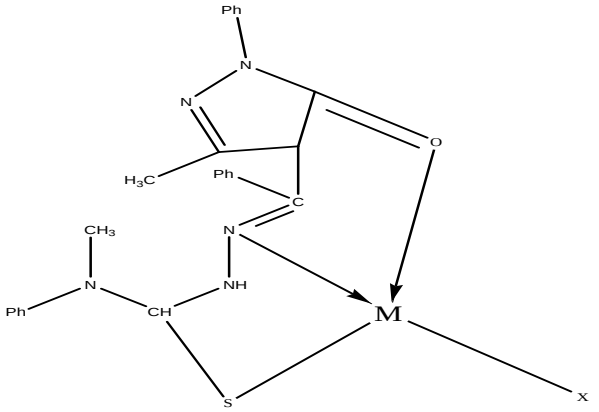

Fig. 5: Proposed structure of complex M(HL)X (4, 5).
Where M = Cu (II), X = Cl^-, NO_3^-.

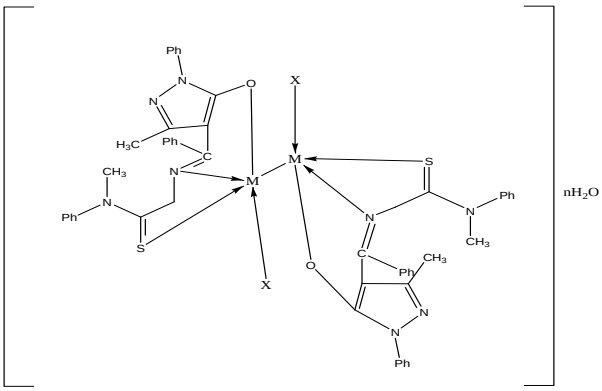

Fig. 6: Proposed structure of complex $(ML)_2$ X_2 (6, 8 and 9).
Where M = Zn (II), Cu(II).

ACKNOWLEDGMENTS

The authors are grateful to KFRI, Peechi, Thrissur, Kerala, India for elemental analyses. We are thankful to SAIF Cochin, Kerala, India for providing NMR results. We are also thankful to SAIF IIT Madras, India for providing EPR result. We are also thankful to Department of Botany, The Zamorin's Guruvayurappan college, Calicut and Department of Biotechnology and Microbiology, School of life sciences, Thalassery Campus for providing laboratory facility to do antimicrobial studies. The University Grants Commission (UGC) India is also gratefully acknowledged for financial support.

REFERENCES

1. Bindu, P.; Kurup, M.R.P.; Satyakeerty, T.R. EPR, cyclic voltammetric and biological activities of copper (II) complexes of salicylaldehyde N (4)-substituted thiosemicarbazone and heterocyclic bases. *Polyhedron*, 1999; 18: 321–331.
2. D. X. West, G.A. Bain, R.J. Butcher, J.P. Jasinki, Y. Li, R.Y. Pozdniakiv, J .Valdez-Martinez, R.A. Toscano, S.H. Ortega, Structural studies of three isomeric forms of heterocyclic N (4)-substituted thiosemicarbazones and two nickel (II) complexes *Polyhedron*, 1996; 15: 665-674.
3. C. R. Kowol, R. Berger, R. Eichinger, A. Roller, M. A. Jakupec, P. P. Schmidt, V. B. Arion, B. K. Keppler, Gallium (III) and iron (III) complexes of alpha-N- heterocyclic thiosemicarbazones: synthesis, characterization, cytotoxicity, and interaction with ribonucleotide reductase. .*J. Med. Chem*, 2007; 50: 1254–1265.
4. Hall, M. D.; Brimacombe, K. R.; Varonka, M. S.; Pluchino, K. M.; Monda, J. K.; Li, J.; Walsh, M. J.; Boxer, M. B.; Warren, T. H.; Fales, H. M.; Gottesman, M. M. Synthesis and Structure–Activity Evaluation of Isatin-β-thiosemicarbazones with Improved Selective Activity toward Multidrug-Resistant Cells Expressing P-Glycoprotein *J. Med. Chem*, 2011; 54: 5878–5889.
5. Mouayed A. Hussein, Muhammad Adnan Iqbal, Muhammad Asif, Rosenani A. Haque, Mohammed B. Khadeer Ahamed, Amin M. S. Abdul Majid, Teoh Siang Guan, Asynthesis, Crystal Structures and in Vitro Anticancer Studies of New Thiosemicarbazone Derivatives, Phosphorus, Sulfur Silicon Relat. Elem., 2015; 190: 1498-1508.
6. S. Gelin, B. Chantegrel, A.I. Nadi, Synthesis of 4-(acylacetyl)-1-phenyl-2-pyrazolin- 5-ones from 3-acyl- 2H-pyran-2, 4(3H)-diones. Their synthetic applications to functionalized 4-oxopyrano [2, 3-c] pyrazole derivatives *J. Org.Chem.*, 1983; 48: 4078–4082.
7. Yuting Zhong, Lang Liu, Guangfei Liu, Dongling Wu, Jixi Guo, Dianzeng Jia Crystal structure and photoisomerism of 1-phenyl-3-methyl-4-(4-fluorobenzal)-5-pyrazolone 4-methylthiosemicarbazone in the solid state *J. Mol. Struct.*, 2008; 889: 259–264.
8. S. Jayasree, K.K. Aravindakshan Structural and antitumour studies of metal complexes with thiosemicarbazones of β-diketoesters, *Polyhedron*, 1993; 10: 1187-1192.
9. S. Jayasree, KK Aravindakshan - Synthesis, characterization and antitumour studies of metal chelates of acetoacetanilide thiosemicarbazone *Transition Met, Chem*, 1993; 18(1): 85-88.
10. J. P. Scovill, D.L. Klayman, C. F. Franchino, 2-Acetylpyridine thiosemicarbazones. 4. Complexes with transition metals as antimalarial and antileukemic agents, J. Med. Chem, 1982; 25: 1261-1264.
11. B.S. Jensen, The Synthesis of 1-phenyl-3-methyl-4-acyl-pyrazol-5ones, Acta Chem. Scand, 1959; 13: 1668-1670.
12. A.W. Bauer, W.M. Kirby, J.C. Sherris, M. Turck Antibiotic susceptibility testing by a standardized single disk method. Am J Clin Pathol, 1966; 45(4): 493–496.
13. H.L. Singh, A.V. Varshney, Synthetic, structural, and biochemical studies of organotin (IV) with Schiff bases having nitrogen and sulphur donor ligands. Bioinorg. Chem. Appl., 2006; 7: 2006-2013.
14. D.X. West, J.S. Ives, G.A. Bain, A.E. Liberta, J. Valdes-Martinez, K.H. Ebert, S. H- Ortega, Copper(II) and nickel (II) complexes of 2, 3-butanedione bis(N(3)-substituted thiosemicarbazones) *Polyhedron*, 1997; 16: 1895–1905.
15. B. Gray, C.J. Ballhausen, A Molecular Orbital Theory for Square Planar Metal Complexes *J. Am. Chem. Soc.*, 1963; 85: 260-265.
16. M. Silverstein, G. C. Bassler, C. Morril, Spectroscopic Identification of Organic Compounds, John Wiley, Newyork, 1981.
17. S. Renjusha, M.R.P. Kurup, Structural and spectral studies on manganese (II) complexes of di-2-pyridyl ketone N (4) - methyl and N (4)-ethyl thiosemicarbazones, *Polyhedron*, 2008; 27: 3294-3298.
18. R. S. Joseyphus, M.S. Nair, Antibacterial and antifungal studies on some Schiff base complexes of zinc (II). *Mycology*, 2008; 36: 93–98.